Robles Martínez, Á.; Ruano García, MV.; Ribes Bertomeu, J.; Ferrer, J. (2013). Performance of industrial scale hollow-fibre membranes in a submerged anaerobic MBR (HF-SAnMBR) system at mesophilic and psychrophilic conditions. Separation and Purification Technology. (104):290-296. doi:10.1016/j.seppur.2012.12.004.

Performance of industrial scale hollow-fibre membranes in a submerged anaerobic MBR (HF-SAnMBR) system at mesophilic and psychrophilic conditions

A. Robles[a,*], M.V. Ruano[b], J. Ribes[b], and J. Ferrer[a]

[a] Institut Universitari d'Investigació d'Enginyeria de l'Aigua i Medi Ambient, IIAMA, Universitat Politècnica de València, Camí de Vera s/n, 46022, València, Spain. (E-mail: *ngerobma@upv.es; jferrer@hma.upv.es*)

[b] Departament d'Enginyeria Química, Escola Tècnica Superior d'Enginyeria, Universitat de València, Avinguda de la Universitat s/n, 46100, Burjassot, València, Spain. (E-mail: *m.victoria.ruano@uv.es; josep.ribes@uv.es)*

* Corresponding author: Tel.: +34 96 387 99 61; Fax: +34 96 387 90 09 E-mail: *ngerobma@upv.es*

Abstract

The aim of this work was to evaluate the effect of temperature on the performance of industrial hollow-fibre (HF) membranes treating urban wastewater in a submerged anaerobic MBR system (SAnMBR). To this end, a demonstration plant with two commercial HF ultrafiltration membrane modules (PURON®, Koch Membrane Systems, PUR-PSH31) was operated at 20, 25 and 33 ºC. The mixed liquor total solid (MLTS) level was a key factor affecting membrane permeability (K). K was higher under psychrophilic than mesophilic conditions when operating at similar transmembrane fluxes and MLTS, because the biomass activity of the psychrophilic mixed liquor was lower than the mesophilic mixed liquor. Thus, lower extracellular polymeric substances (EPS) and soluble microbial products (SMP) levels were observed at psychrophilic conditions, which affected not only the three-dimensional floc matrix, but also the fouling propensity. However, no chemical cleaning was needed during the experimental period (almost one year) because no irreversible fouling problems were detected.

Keywords

Extracellular polymeric substances (EPS); industrial hollow-fibre membranes; membrane permeability; mesophilic and psychrophilic anaerobic conditions; soluble microbial products (SMP).

1. Introduction

Aerobic membrane bioreactors (MBR) have recently become not only a legitimate alternative to conventional activated sludge processes, but also the preferred choice for urban wastewater treatment because of their reliability and efficiency [1]. The quality of the effluent is very good but the operating costs of aeration and sludge handling remain the biggest drawbacks of aerobic MBR technology [2]. High energy demand and high waste generation are both at odds with sustainability principles.

In this respect, in recent years there has been increasing interest in the study of anaerobic urban wastewater treatment at ambient temperatures, mainly focused on the sustainability benefits of anaerobic processes as opposed to aerobic processes (lower sludge production, lower energy demands, and energy recovery from methane production). The main challenge of anaerobic biotechnology is to develop treatment systems, such as anaerobic membrane bioreactors (AnMBR) that prevent biomass loss and enable high sludge retention times (SRTs) in order to compensate for the low growth rates of anaerobic microorganisms at ambient temperatures [3]. However, operating membrane bioreactors at high SRTs may imply operating at high MLTS levels. This is considered to be one of the main constraints on membrane operating [4] because it can result in a higher membrane fouling propensity.

Besides MLTS levels, several sludge properties have been identified elsewhere as key factors that affect membrane performance (because they can lead to the onset of either irreversible or irrecoverable fouling), i.e. particle size distribution, extracellular polymeric substances (EPS), soluble microbiological products (SMP), and biomass concentration [5]. Moreover, the limitations of anaerobic metabolism at ambient temperatures can cause non-complete organic matter degradation, leading to an increase in colloidal and soluble components that increase the fouling propensity of membranes [6]. Threshold EPS have been reported not only as the major sludge component keeping the floc in a three-dimensional matrix, but also as a key membrane foulant in MBR systems [7, 8, 9]. On the other hand, it is widely accepted that EPSs and SMPs are identical concepts [1], and that SMPs easily accumulate in MBRs because they are absorbed on the membrane surface where they block membrane pores and reduce membrane permeability [10]. Moreover, SMPs influence the structure and porosity of the cake layer formed on membrane surface [11]. Both EPSs and SMPs have been directly related to the biomass concentration of the mixed liquor [12], as well as to operating SRT [13]: a key factor in anaerobic biomass growth at ambient temperatures.

Several published studies have evaluated the effect of different sludge properties on membrane fouling in SAnMBR technology on a laboratory scale [3, 4, 14, 15]. However, there is still a lack of knowledge about the assessment of the different fouling mechanisms in SAnMBR technology treating low-strength wastewaters on an industrial scale. Moreover, the effect of the main operating conditions on membrane fouling has not been adequately evaluated on a laboratory scale because it depends considerably on the membrane size, especially in the case of hollow-fibre (HF) membranes. Therefore, further research is needed on HF-SAnMBR technology with industrial scale membranes in order to facilitate the design and implementation of this technology in full-scale

WWTPs.

The main objective of this paper was to study the effect of temperature on the performance of industrial hollow-fibre membranes. This study is innovative because it studies membrane performance under specific conditions similar to those expected in full-scale plants located in warm climate regions (e.g. Mediterranean ones). In this respect, this study shows the long-term performance of industrial HF membranes at mesophilic and psychrophilic conditions in an SAnMBR demonstration plant treating effluent from a pre-treatment WWTP. The SAnMBR plant is located in Valencia (Spain), where the average daily ambient temperature ranges from 15 and 35 ºC approx. during the year. The assessment of the impact of temperature upon membrane performance will shed more light on the possible applications of this technology in the treatment of urban wastewater at ambient temperatures.

2. Materials and methods

2.1. Demonstration plant description

Figure 1 shows the flow diagram of the HF-SAnMBR demonstration plant used in this study. It consists of an anaerobic reactor with a total volume of 1.3 m^3 (0.4 m^3 head space) connected to two membrane tanks each with a total volume of 0.8 m^3 (0.2 m^3 head space). Each membrane tank has one industrial HF ultrafiltration membrane unit (PURON®, Koch Membrane Systems (PUR-PSH31) with 0.05 µm pores). Each module has 9 HF bundles, 1.8 m long, giving a total membrane surface of 30 m^2. In order to improve the stirring conditions of the anaerobic reactor and to favour the stripping of the produced gases from the liquid phase, a fraction of the produced biogas is

continuously recycled to this reactor. In order to minimise the cake layer formation, another fraction of the produced biogas is also continuously recycled to the membrane tanks through the bottom of each fibre bundle. To recover the bubbles of biogas in the permeate leaving the membrane tank, two degasification vessels (DV) were installed: each one between the respective MT and the vacuum pump. The funnel-shaped section of conduit makes the biogas accumulate at the top of the DV. The resulting permeate is stored in the clean-in-place (CIP) tank. In order to control the temperature when necessary, the anaerobic reactor is jacketed and connected to a water heating/cooling system.

Normally membranes are operated according to a specific schedule involving a combination of different individual stages taken from a basic filtration-relaxation (F-R) cycle. In addition to the classical membrane operating stages (filtration, relaxation, and back-flush), two additional stages of membrane operation were also considered (degasification and ventilation). Degasification stage consists of a period of high flow-rate filtration that is carried out to enhance the filtration process efficiency by removing the accumulated biogas from the top of the dead-end fibres. In the ventilation stage, permeate is pumped into the membrane tank through the degasification vessel instead of through the membrane. The aim of ventilation stage is to recover the biogas accumulated in the degasification vessel. Thus, in terms of membrane cleaning, ventilation performs as a relaxation stage since no transmembrane flux is applied whilst maintaining a given gas sparging intensity.

By using two membrane tanks in parallel, the plant was designed with high operating flexibility, which allows working with either one membrane tank or both tanks. Moreover, each tank allows recycling continuously the obtained permeate to the

anaerobic reactor. Specifically in this study, the obtained permeate from MT1 (see Figure 1) was continuously recycled to the system in order to test different J_{20} without affecting the hydraulic retention time (HRT) of the process. On the other hand, the obtained permeate from MT2 was fed to the CIP tank and corresponds to the effluent wastewater of the system (see Figure 1). Hence, different operating filtration modes were set in MT2 to achieve the different HRTs that were programmed to assess the biological process performance.

Numerous on-line sensors and automatic devices were installed in order to automate and control the plant operation and provide on-line information about the state of the process. In particular a group of on-line sensors was assigned to each membrane tank consisting of: 1 pH-temperature transmitter; 1 level indicator transmitter; 1 flow indicator transmitter for the mixed liquor feed pump; 1 flow indicator transmitter for the permeate pump; and 1 liquid pressure indicator transmitter in order to control the TMP. The group of actuators assigned to each membrane tank consisted of a group of on/off control valves that determine the direction of the flow in order to control the different membrane operating stages (filtration, back-flush, relaxation…) plus 3 frequency converters. Each frequency converter controls the rotating speed of the permeate pump, the mixed liquor feed pump, and the membrane tank blower. Further details about this SAnMBR demonstration plant can be found in Giménez *et al*. [16].

2.2. Demonstration plant operation

The SAnMBR demonstration plant was operated at a constant SRT of 70 days and three different temperatures (20, 25 and 33 ºC). The pH of the mixed liquor remained relatively stable at around 6.75 (the pH ranged from 6.5 to 7), and the alkalinity of the

mixed liquor remained at values of approximately 600 mg$CaCO_3$ L^{-1}. During the experimental period, the usual membrane operating mode was as follows: a 300-second basic F-R cycle (250 s filtration and 50 s relaxation), 30 seconds of back-flush every 10 F-R cycles, 40 seconds of ventilation every 10 F-R cycles, and 30 seconds of degasification every 50 F-R cycles. The up-flow sludge velocity in the membrane surface was set to 2.7 mm s^{-1}; and the average specific gas demand per square metre of membrane (SGD_m) was 0.23 Nm^3 m^{-2} h^{-1} (corresponding to a gas sparging velocity of around 7 mm s^{-1}) . The operating period shown in this work was divided into four experimental periods taking into account both the 20 ºC-normalised transmembrane flux (J_{20}) and the controlled temperature values studied. Table 1 summarises the average values for J_{20}, 20 ºC-normalised critical flux ($J_{C,20}$), temperature and HRT in each experimental period. As mentioned before, the J_{20} values were set by using MT1, whilst the HRT values were set by using MT2.

Table 2 shows the average wastewater characteristics of the influent entering the anaerobic reactor. This table highlights the significant influent sulphate levels, and also the wide variation in the influent loads, reflected by the high standard deviation of each parameter. The uncertainty associated with each value includes both the standard deviation of the different samples analysed throughout the experiment and the variation coefficient associated with the analytical methods.

2.3. Analytical methods

2.3.1. Water quality analysis

In addition to monitoring the process on-line, the performance of the biological

process was assessed by taking 24-hour composite samples from influent and effluent streams, and taking grab samples of biogas and anaerobic sludge once a day. The following parameters were analysed in influent, effluent and anaerobic sludge: total solids (TS); volatile solids (VS); total suspended solids (TSS); volatile suspended solids (VSS); volatile fatty acids (VFA); carbonate alkalinity (Alk); sulphate (SO_4-S); total sulphide (measured as HS^-); nutrients (ammonium (NH_4-N) and orthophosphate (PO_4-P)); and total and soluble chemical oxygen demand (COD_T and COD_S, respectively). Particle size distribution, and EPS and SMP levels were measured twice a month. Furthermore, a sludge sample was fixed for microbiological analysis once a week.

Solids, COD, sulphate, sulphide and nutrients were determined according to Standard Methods [17]. Alk and VFA levels were determined by titration according to the method proposed by WRC [18].

2.3.2. Floc structure and particle size distribution

Particle size distribution was measured twice a month using a MASTERSIZER2000 coupled to Hydro 2000SM (A) with a detection range of 0.02 to 2000 µm. The sludge floc was examined by light microscopy and the images were captured with a microscope Leica DM2500 and a Leica DFC420c digital camera.

2.3.3. Microbiological analysis

Microbiological analysis was performed once a week by using the FISH (fluorescent in situ hybridization) technique [19] to identify the different species of sulphate reducing bacteria (SRB) and methanogenic archaea (MA). Hybridized cells

were enumerated by capturing images with a Leica DM2500 epifluorescence microscope and a Leica DFC420c digital camera and using automated bacteria quantification software [20] programmed in Matlab®. Further details about the microbiological analysis approach can be found in Giménez *et al*. [21].

2.3.4. EPS and SMP extraction and measurement

EPS and SMP extraction and measurement were carried out twice a month. Mixed liquor was collected from the membrane tank and a sample of 150 mL was centrifuged at 2000xG for 15 min at 4 ºC (Eppendorf Centrifuge 5804R). The supernatant was filtered with a 1.2 µm filter and the SMP levels (SMP_C and SMP_P, related to carbohydrates and proteins, respectively) were measured. The EPS extraction was based on the Cation Exchange Resin (CER) method proposed by Frølund *et al.* [22]. The sludge pellets were resuspended to their original volume using a buffer consisting of 2 mM Na_3PO_4, 4 mM NaH_2PO_4, 9 mM NaCl and 1 mM KCl at pH 7. The EPS extraction was performed as follows: 100 mL of the suspension was transferred to an extraction container and 70 g/g MLVS of CER were added; the suspension was stirred at the selected intensity (900 rpm) and extraction time (20 hours) at 4 ºC. The extracted EPS was harvested by centrifuging the CER/sludge suspension for 15 min at 12000xG and 4 ºC to remove the CER and MLTS. The supernatant was taken and filtered with a 1.2 µm filter and the extracted EPS levels ($eEPS_C$ and $eEPS_P$, related to carbohydrates and proteins, respectively) were measured. The carbohydrates and proteins of both SMP and eEPS were determined by colorimetry according to the methodology proposed by Dubois *et al*. [23] and Lowry *et al*. [24], respectively. Bovine serum albumin (BSA) and glucose were used as protein and carbohydrate standards, respectively.

2.3.5. Membrane performance indices

The 20 ºC-normalised membrane permeability (K_{20}) was calculated using a simple filtration model (Eq. 1) that takes into account the TMP and J values monitored on line. This simple filtration model includes a temperature correction (Eq. 2) to take into account the dependence of permeate viscosity on temperature. The same temperature correction was used for J (Eq. 3). The total membrane resistance (R_T) was represented theoretically by the following partial resistances (Eq. 4): membrane resistance (R_M); cake layer resistance (R_C); and irreversible layer resistance (R_I).

$$K_{20} = \frac{J_T f_T}{TMP} \quad \text{(Eq. 1)}$$

$$f_T = e^{-0.0239\,(T-20)} \quad \text{(Eq. 2)}$$

$$J_{20} = J_T \cdot e^{-0.0239\,(T-20)} \quad \text{(Eq. 3)}$$

$$R_T = R_M + R_C + R_I \quad \text{(Eq. 4)}$$

Moreover, a modified flux-step method [25] was carried out in order to determinate the $J_{C,20}$ of each operating interval. Each $J_{C,20}$ was calculated according to the weak definition of this concept, i.e. the flux above which the relationship between J_{20} and TMP becomes non-linear. Table 1 shows the obtained results for $J_{C,20}$ in each experimental period. These values were obtained at 23 g L^{-1} of MLTS and SGD_m of 0.23 $Nm^3\ h^{-1}\ m^{-2}$.

3. Results and discussion

263 *3.1. Long-term membrane performance at mesophilic and psychrophilic conditions*

264

265 Table 1 shows the obtained results for $J_{C,20}$ in each experimental period (determined
266 at 23 g L^{-1} of MLTS and SGD_m of 0.23 Nm^3 h^{-1} m^{-2}). For instance, on day 125 and day
267 240, $J_{C,20}$ resulted in 14 LMH in both trials. Therefore, the critical flux remained
268 generally at values over 14 LMH during the operating period since SGD_m was
269 maintained at 0.23 Nm^3 h^{-1} m^{-2} and MLTS remained generally below 23 g L^{-1} (see days
270 1-125 and 240-310). Hence, the long-term operating shown in this study was mainly
271 carried out at sub-critical filtration conditions since J_{20} was varied from 10 to 13.3 LMH
272 [26].

273

274 Figure 2 shows the average daily K_{20} (calculated with Eq. 1 and Eq. 2) obtained
275 during the operating period, and the average daily MLTS level in the anaerobic sludge
276 entering the membrane tank. Notice that the MLTS level in the membrane tank
277 increases in proportion to the ratio between the net permeate flow rate and the sludge
278 flow rate entering the membrane tank. Therefore, the operating MLTS in the membrane
279 tank was actually higher (up to 5 g L^{-1}) than the ones shown in this work, since the data
280 presented correspond to the MLTS level entering the membrane tank.

281

282 Figure 2 shows the considerable extent to which the MLTS level affects K_{20} in the
283 four experimental periods in this study (the MLTS decrease observed on day 170 was
284 caused by a problem in the sludge wasting system). Every variation of the MLTS level
285 was inversely reflected on K_{20}. It is important to note that even at high MLTS levels (up
286 to 25 g L^{-1}), K_{20} remained at sustainable values. As can be seen in period ii, K_{20}
287 remained at values above 100 LMH bar^{-1} until a MLTS level of around 25 g L^{-1} was
288 reached. Similar behaviour was observed in period iii. This figure also shows that at

relatively stable MLTS levels (see days 90 - 110 or days 120 - 135), K_{20} remained quite stable. This K_{20} stability could be due to the low TMP achieved during this period (below 0.1 bars), which minimises membrane compression and causes a stable R_M. Moreover, as can be observed in period iv, K_{20} improved when MLTS decreased, which indicates the absence of irreversible fouling components on R_T. Hence, the higher K_{20} obtained during the first months of operation was related to a lower cake layer formation rate due to lower MLTS levels. It is important to highlight the two different effects that determine R_C: the cake layer formation rate (due to the filtration process) and the cake layer removal rate (due mainly to biogas sparging). It is well known that at a given SGD_m the cake layer removal efficiency decreases when the MLTS level increases. Therefore, in our study, which was carried out at a constant SGD_m, the decrease in K_{20} caused by a higher MLTS level was mainly due to an increase in the cake layer formation rate. However, no irreversible fouling was detected, mainly as a result of both working at sub-critical filtration conditions and establishing an adequate membrane operating mode.

Figure 2 shows the different membrane performances in period i (mesophilic conditions) and period iv (psychrophilic conditions), which were conducted at identical J_{20}. Similar K_{20} values were achieved even though membranes operated at higher MLTS levels in period iv than in period i. This behaviour can be observed better in Figure 3.

3.2. Sludge properties affecting membrane performance at mesophilic and psychrophilic conditions

3.2.1. Effect of MLTS on membrane performance

315 Figure 3 shows how the MLTS level affects K_{20} in three of the four series carried
316 out during different operating periods. As can be observed in this figure, under the
317 selected operating conditions (0.23 $Nm^3 h^{-1} m^{-2}$ of SGD_m), a linear dependency of K_{20}
318 on MLTS was observed for each J_{20}. Any increase in the MLTS level caused a
319 proportional decrease in K_{20}. As this figure illustrates, the behaviour in the two
320 experimental series carried out at 33 ºC (13.3 and 10 LMH of J_{20}) is similar since both
321 series were carried out at the same mesophilic operating conditions. Despite observing
322 no clear differences between the two series conducted at mesophilic conditions, it can
323 be concluded that at similar MLTS levels the higher the J_{20} applied the lower the K_{20}
324 obtained. This difference can also be observed in the slope of the linear regression
325 between the MLTS level and K_{20}. This slope was slightly higher with a J_{20} of 13.3 LMH
326 than of 10 LMH, which indicated a higher reversible fouling propensity at higher fluxes.
327 Moreover, both mathematical equations seem to indicate that the dependency of K_{20} on
328 MLTS starts becoming independent of J_{20} when the MLTS level tends to zero since both
329 intercept terms present similar values. On the contrary, the impact of J_{20} on K_{20} gets
330 higher as MLTS increases. This behaviour tallies well with the classical definition of
331 membrane permeability treating pure water. On the other hand, Figure 3 shows clear
332 differences in the resulting K_{20} between both mesophilic and psychrophilic conditions.
333 In this respect, K_{20} is considerably higher when the system is operated at psychrophilic
334 than at mesophilic conditions. For instance, as can be deduced from the slope of the
335 linear regressions resulting from the experimental series conducted at 13.3 LMH, K_{20} is
336 more sensitive to changes in MLTS when operating at 20 ºC than at 33 ºC. Figure 3
337 illustrates that the differences in K_{20} observed between mesophilic and psychrophilic
338 conditions are higher when the MLTS level decreases. In contrast, when the MLTS
339 level increases, this parameter becomes a key factor affecting membrane performance in
340 the operating conditions studied. Hence, it is possible to state that the influence of

MLTS on K_{20} under mesophilic and psychrophilic operating conditions is also conditioned by other operating factors.

3.2.2. Effect of particle size distribution on membrane performance

Figure 4 shows the distribution of the average particle size in the mixed liquor corresponding to the three temperatures studied. For each temperature period, only one distribution is shown since the mean particle size throughout each temperature period depicted the same distribution shape. As can be seen in this figure, a unimodal floc size distribution was observed in every experimental period, which indicates that only one population of aggregates was present in the sludge. As ascertained by other authors [4], the single-peak distribution was demonstrated by microscopic observations of the flocs in the mixed liquor (see Figure 5). In these microscopic observations, a large amount of fine flocs in the mixed liquor was not observed. Thus, a low membrane fouling propensity, i.e. a low probability of permeability decrease, was expected [4, 27]. However, a slight decrease in the average value of these unimodal floc size distributions was detected when the temperature was reduced. These results were corroborated by examining the flocs in the mixed liquor by light microscopy. The mean floc sizes observed under psychrophilic conditions were smaller than those observed at mesophilic ones. Therefore, at psychrophilic conditions lower cake layer porosities may be reached as a result of the small average particle sizes. Moreover, as a result of the operating pressure, lower cake layer porosities may lead to higher cake layer tortuosity, which implies a higher specific cake layer resistance [28]. Nevertheless, Figure 4 shows that no particles lower than 0.3 μm were detected. Hence, considering that the mean pore size of the membranes is 0.05 μm, these results predict that, for our case study, this decrease of the particle sizes due to the decrease of temperature could only affect the

cake layer formation and/or consolidation over the membrane surface, but no other membrane filtration resistances related to MLTS, such as the one related to the internal fouling due to the blockage of pore channels.

3.2.3. Effect of biomass population, and EPS and SMP compounds on membrane performance

Figure 5 shows a sample of the microscopic observations of floc size and structure in the mixed liquor under mesophilic (Figure 5a) and psychrophilic (Figure 5b) conditions. This figure illustrates that the mean floc size in the mixed liquor was lower under psychrophilic conditions (approx. from 25 to 100 μm) than under mesophilic conditions (approx. from 50 to 200 μm). This reduction in floc size can be attributed to the impact of temperature upon the anaerobic biomass growth rate. Since the SRT was set constant to 70 days throughout the operating period, biomass activity declined sharply when the temperature was decreased (see Table 3). Thus, lower biomass concentrations were detected under psychrophilic conditions, which resulted in a lower enzymatic activity that could affect the sludge conglomeration.

Table 3 shows the average values derived from the anaerobic biomass activity in both mesophilic and psychrophilic operating periods. The uncertainty associated with each value includes both the standard deviation of the different samples analysed throughout the experimental period and the coefficient of variation associated with the analytical methods. This table shows a lower biomass concentration (referred to SRB and MA) at psychrophilic conditions than at mesophilic ones. This lower biomass concentration resulted in a considerably lower concentration of EPS in the mixed liquor, and also a lower SMP production. It is important to note that the EPS level is considered

393 to be one of the main sludge components that keeps the floc in a three-dimensional
394 matrix. This fact was also observed in Figure 5, i.e. the average sizes of the
395 psychrophilic flocs were lower than the mesophilic flocs, probably as a result of the
396 lower EPS levels shown in Table 3.
397
398 Table 3 shows a considerably higher fraction of proteins than carbohydrates in both
399 eEPS and SMP. The protein (P)/carbohydrate (C) ratio of SMP was 16.4 and 7.0 for
400 mesophilic and psychrophilic sludge, respectively. The P/C ratio of eEPS was 3.6 and
401 3.1 for mesophilic and the psychrophilic sludge, respectively. Liao *et al*. [29] observed
402 that an increase in the P/C ratio resulted in an increase of the hydrophobicity of the floc,
403 thus increasing the cake layer formation propensity. Since no clear differences were
404 observed in the eEPS-P/C ratios, it was assumed that this parameter made no critical
405 contribution to the differences observed in this study concerning the consolidation of the
406 cake layer upon the membrane surface under mesophilic and psychrophilic conditions.
407 A considerable difference was, however, observed between both SMP-P/C ratios under
408 mesophilic and psychrophilic conditions (more than double). Therefore, the SMP level
409 (and SMP_P particularly) was identified as one key factor affecting K_{20} in this work.
410 Pollice *et al*. [12] established that there is proportionality between biomass
411 concentration and SMP production due to the increased release of organic material from
412 cell lysis. In this sense, results from Table 3 show both higher biomass concentrations
413 and higher SMP and eEPS levels under mesophilic conditions than under psychrophilic
414 conditions. It is well known that the amount of SMP and EPS in mixed liquor directly
415 affects membrane permeability. This effect was also observed in our study because
416 lower values of K_{20} were reached when the SMP and eEP_C levels in the mixed liquor
417 were higher, i.e. at higher temperatures. Moreover, Huang *et al*. [10] observed that the
418 SMP could induce inter-particle pore blocking when they pass through the cake layer,

resulting in a higher cake layer formation rate. In this respect, a given gas sparging intensity could be less effective in detaching the cake layer from the membrane surface when there is a higher SMP level in the system, as a result of a higher propensity of cake layer formation and consolidation upon the membrane surface [7]. In addition, some studies have shown that when membranes are operated at sub-critical filtration conditions (as in our study), SMP and EPS are the main factors affecting membrane fouling since these compounds are accumulated in the system [12].

Hence, the differences observed in this study between K_{20} under mesophilic and psychrophilic operating conditions can be explained by a higher fouling propensity at mesophilic than psychrophilic conditions due to a higher biomass concentration resulting in higher SMP and eEPS levels in the mixed liquor. In either case, since the level of EPS and SMP in the mixed liquor influences the structure and porosity of the cake layer created over the membrane surface [11], this higher fouling propensity was related to the reversible cake layer resistance. This hypothesis was strengthened because the K_{20} returned to its previous values when the MLTS level decreased.

3.2.4. Other factors minimising the onset of irreversible fouling problems

As it has been mentioned before K_{20} returned to initial values when the MLTS concentration decreased (see Figure 2). The recovery of K_{20} was achieved without any chemical cleaning of the membrane. Hence, after almost one year of operation, no irreversible fouling problems were detected, even with high MLTS and temperature shocks affecting biomass population and its derived compounds. Moreover, it is important to highlight that the total filtering resistance remained at similar values throughout the whole operating period, when operating at similar MLTS levels. The

445 total filtering resistance was $1.5 \cdot 10^{12}$ m^{-1} in average. Further details on the absence of
446 irreversible fouling in this system can be found in Robles *et al.* [26].
447
448 Apart from operating at sub-critical filtration conditions and establishing an
449 adequate membrane operating mode, no chemical cleaning was necessary probably
450 because of the pH of the mixed liquor, which was always kept at values below 7 by
451 recycling the biogas produced for in-situ sparging purposes (i.e. the CO_2 remained in
452 the mixed liquor, resulting in alkalinity values of approx. 600 $mgCaCO_3$ L^{-1}). pH values
453 below 7 may result in a negligible formation of chemical precipitates (e.g. struvite),
454 which favours the absence of chemical fouling problems [26]. Low pH indirectly means
455 low fouling propensity due to low dispersion of sludge flocs resulting in sub-products
456 generation directly related to biofouling, i.e. colloids and solutes or biopolymers [30].
457 Moreover, it has been observed that low pH levels result in a low adherence and fouling
458 propensity of EPS [31]. Nevertheless, further research is needed in order to assess the
459 actual effect of pH on membrane fouling in anaerobic systems.
460
461 *3.3. Overall biological process performance*
462
463 The SAnMBR plant was operated at a SRT of 70 days and the HRT was ranged
464 from approx. 5 to 24 hours. As regards the COD removal efficiency no significant
465 differences were observed under both mesophilic and psychrophilic operating
466 conditions, taking also into account the considerable dynamics in the influent load.
467 COD removal efficiencies of around 85 % and low effluent COD concentrations (< 100
468 mg L^{-1}) were achieved. No significant differences were observed throughout the period,
469 mainly due to the high retention of solids achieved by the physical process and the
470 significant operating SRT. On the other hand, the decrease in the temperature resulted in

471 an increase in the average sludge production (approx. 30%): from about 0.16 to 0.23 kg
472 VS kg^{-1} $COD_{REMOVED}$. This increase was attributed to the decline of the biomass activity
473 observed when the temperature was reduced, particularly due to a decrease in the
474 hydrolysis rate. This decrease in the hydrolysis rate resulted in an accumulation of
475 solids in the system. Nevertheless, the sludge production at psychrophilic temperature
476 conditions was still lower than the common values observed in aerobic treatment of
477 urban wastewaters (≈ 0.5 kg VS kg^{-1} $COD_{REMOVED}$). Concerning the biogas production,
478 the decrease in the temperature resulted in a decrease in the methane production
479 (approx. 20%), which was also related to the decrease in the hydrolysis rate.
480 Nevertheless, a significant average biogas production (around 100 L d^{-1}) was observed
481 throughout the whole experimental period, which evidenced a suitable biological
482 process performance under both mesophilic and psychrophilic operating conditions.
483 Regarding the sulphate reducing activity, influent sulphate was almost completely
484 reduced to sulphide for the whole operating period (around 95%). It resulted in a
485 composition of hydrogen sulphide in the biogas of 1.3% in average.
486
487 **4. Conclusions**
488
489 MLTS was identified as one of the key factors that affects K_{20}. Nevertheless, K_{20}
490 remained at sustainable values even at high MLTS (up to 25 g L^{-1}). The floc analysis
491 showed a smaller mean floc size under psychrophilic than under mesophilic conditions,
492 mainly due to a lower biomass activity, and thus lower EPS levels. Higher membrane
493 fouling propensities were observed under mesophilic than under psychrophilic
494 conditions due to higher SMP production. Nevertheless, after almost one year of
495 operating, no irreversible fouling problems were detected. The long-term membrane
496 performance demonstrated that HF-SAnMBR is a promising technology for urban

497 wastewater treatment.

498

499 **Acknowledgements**

500

501 This research work has been supported by the Spanish Research Foundation
502 (CICYT Projects CTM2008-06809-C02-01 and CTM2008-06809-C02-02, and
503 MICINN FPI grant BES-2009-023712) and Generalitat Valenciana (Projects GVA-
504 ACOMP2010/130 and GVA-ACOMP2011/182), which are gratefully acknowledged.

505

506 **References**

507

508 [1] P. Le-Clech, V. Chen, T.A.G. Fane, Fouling in membrane bioreactors used in wastewater treatment, J.
509 Membr. Sci. 284 (2006) 17 – 53.
510 [2] D. Martinez-Sosa, B. Helmreich, T. Netter, S. Paris, F. Bischof, H. Horn, Anaerobic submerged
511 membrane bioreactor (AnSMBR) for municipal wastewater treatment under mesophilic and
512 psychrophilic temperature conditions, Bioresour. Technol. 102 (2011) 10377 – 10385.
513 [3] H.J. Lin, K. Xie, B. Mahendran, D.M. Bagley, K.T. Leung, S.N. Liss, B.Q. Liao, Factors affecting
514 sludge cake formation in a submerged anaerobic membrane bioreactor, J. Membr. Sci. 361 (2010) 126 –
515 134.
516 [4] S. Judd, C. Judd, The MBR Book: Principles and Applications of Membrane Bioreactors for Water
517 and Wastewater Treatment, 2nd edition, Elsevier, ISBN: 978-0-08-096682-3, 2011.
518 [5] H.J. Lin, K. Xie, B. Mahendran, D.M. Bagley, K.T. Leung, S.N. Liss, B.Q. Liao, Sludge properties
519 and their effects on membrane fouling in submerged anaerobic membrane bioreactors (SAnMBRs),
520 Water Res. 43 (2009), 3827 – 3837.
521 [6] M. Herrera-Robledo, D.M. Cid-León, J.M. Morgan-Sagastume, A. Noyola, Biofouling in an anaerobic
522 membrane bioreactor treating municipal sewage, Sep. Purif. Technol. 81 (2011) 49 – 55.
523 [7] S. Tsuneda, H. Aikawa, H. Hayashi, A. Yuasa, A. Hirata, Extracellular polymeric substances
524 responsible for bacterial adhesion onto solid surface, FEMS Microbiology Letters 223 (2003) 287 –
525 292.

526 [8] S. Lyko, D. Al-Halbouni, T. Wintgens, A. Janot, J. Hollender, W. Dott, T. Melin, Polymeric
527 compounds in activated sludge supernatant – Characterisation and retention mechanisms at a full-scale
528 municipal membrane bioreactor, Water Res. 41 (2007) 3894 – 3902.
529 [9] F.G. Meng, S.R. Chae, A. Drews, M. Kraume, H.S. Shin, F.L. Yang, Recent advances in membrane
530 bioreactors (MBRs): membrane fouling and membrane materials, Water Res. 43 (2009) 2405 – 2415.
531 [10] Z. Huang, S.L. Ong, H.Y. Ng, Feasibility of submerged anaerobic membrane bioreactor (SAMBR)
532 for treatment of low-strength wastewater, Water Sci. Technol. 58 (2008) 1925 – 1931.
533 [11] L. Dvořák, M. Gómez, M. Dvořáková, I. Růžičková, J. Wanner, The impact of different operating
534 conditions on membrane fouling and EPS production, Bioresour. Technol. 102 (2011) 6870 – 6875.
535 [12] A. Pollice, A. Brookes, B. Jefferson, S. Judd, Sub-critical flux fouling in membrane bioreactors – a
536 review of recent literature, Desalination 174 (2005) 221 – 230.
537 [13] Y. Lee, C. Jinwoo, Y. Seo, J.W. Lee, K.H. Ahn, Modeling of submerged membrane bioreactor
538 process for wastewater treatment, Desalination 146 (2002) 451 – 457.
539 [14] Z. Huang, S.L. Ong, H.Y. Ng, Submerged anaerobic membrane bioreactors for low-strength
540 wastewater treatment: Effect of HRT and SRT on treatment performance and membrane fouling, Water
541 Res. 45 (2011) 705 – 713.
542 [15] H. Lin, B.Q. Liao, J. Chen, W. Gao, L. Wang, F. Wang, X. Lu, New insights into membrane fouling
543 in a submerged anaerobic membrane bioreactor based on characterization of cake sludge and bulk
544 sludge, Bioresour. Technol. 102 (2011), 2373 – 2379.
545 [16] J.B. Giménez, A. Robles, L. Carretero, F. Durán, M.V. Ruano, M.N. Gatti, J. Ribes, J. Ferrer, A.
546 Seco, Experimental study of the anaerobic urban wastewater treatment in a submerged hollow-fibre
547 membrane bioreactor at pilot scale, Bioresour. Technol. 102 (2011) 8799 – 8806.
548 [17] American Public Health Association/American Water Works Association/Water Environmental
549 Federation, Standard methods for the Examination of Water and Wastewater, 21st edition, Washington
550 DC, USA, 2005.
551 [18] Water Research Commission, University of Cape Town, Simple titration procedures to determine
552 H2CO3* alkalinity and short-chain fatty acids in aqueous solutions containing known concentrations of
553 ammonium, phosphate and sulphide weak acid/bases, Report No. TT 57/92, Pretoria, Republic of South
554 Africa, 1992.
555 [19] R. Amann, B.J. Binder, R.J. Olson, S.W. Chisholm, R., Deveroux, D.A. Stahl, Combination of 16s
556 Ribosomal-RNA-Targeted Oligonucleotide Probes with Flow-Cytometry for Analyzing Mixed

557 Microbial-Populations, App. Environ. Microbiol. 56 (1990), 1919 – 1925.
558 [20] L. Borrás, Microbiological techniques applied to the identification and quantification of
559 microorganisms that are present in EBPR systems (Técnicas microbiológicas aplicadas a la
560 identificación y cuantificación de microorganismos presentes en sistemas EBPR), 2008, PhD Thesis,
561 Departamento de Ingeniería Hidráulica y Medio Ambiente, Universidad Politécnica de Valencia, Spain.
562 [21] J.B. Giménez, L. Carretero, M.N. Gatti, N. Martí, L. Borras, J. Ribes, A. Seco, Reliable method for
563 assessing the COD mass balance of a submerged anaerobic membrane bioreactor (SAMBR) treating
564 sulphate-rich municipal wastewater, Water Sci. Technol. 66 (2012) 494 – 502.
565 [22] B. Frølund, R. Palmgren, K. Keiding, P.H. Nielsen, Extraction of extracellular polymers from
566 activated sludge using a cation exchange resin, Water Res. 30 (1996) 1749 – 1758.
567 [23] M. Dubois, K.A. Gilles, J.K. Hamilton, P.A. Rebers, F. Smith, Colorimetric method for
568 determination of sugar and related substances, Anal. Chem. 28 (1956) 350 – 356.
569 [24] O.H. Lowry, N.J. Rosebrough, A.L. Farr, R.J. Randall, Protein measurement with the folin phenol
570 reagent, J. Biol. Chem. 193 (1951) 265 – 275.
571 [25] A. Robles, M.V. Ruano, F. García-Usach, J. Ferrer, Sub-critical filtration conditions of commercial
572 hollow-fibre membranes in a submerged anaerobic MBR (HF-SAnMBR) system: The effect of gas
573 sparging intensity, Bioresour. Technol. 114 (2012) 247–254.
574 [26] A. Robles, M.V. Ruano, F. García-Usach, J. Ferrer, Sub-critical long-term operation of industrial
575 scale hollow-fibre membranes in a submerged anaerobic MBR (HF-SAnMBR) system, Sep. Purif.
576 Technol. 100 (2012) 88 – 96.
577 [27] H.Y. Ng, S.W. Hermanowicz, Specific resistance to filtration of biomass from membrane bioreactor
578 reactor and activated sludge: effects of exocellular polymeric substances and dispersed microorganisms,
579 Water Environ. Res. 77 (2005) 187 – 192.
580 [28] A.A. Merdaw, A.O. Sharif, G.A.W. Derwish, Mass transfer in pressure-driven membrane separation
581 processes, Part I, Chem. Eng. J. 77 (2011) 215 – 228.
582 [29] B.Q. Liao, D.G. Allen, I.G. Droppo, G.G. Leppard, S.N. Liss, Surface properties of sludge and their
583 role in bioflocculation and settleability, Water Res. 35 (2001) 339 – 350.
584 [30] W.J. Jane Gao, H.J.Lin, K.T. Leunga, B.Q. Liao, Influence of elevated pH shocks on the
585 performance of a submerged anaerobic membrane bioreactor, Process Biochem. 45 (2010) 1279 – 1287.
586 [31] A. Sweity, W. Ying, S. Belfer, G. Oron, M. Herzberg, pH effects on the adherence and fouling
587 propensity of extracellular polymeric substances in a membrane bioreactor, J. Membr. Sci. 378 (2011)

186 – 193.

Table and figure captions

Table 1. Average values for the 20 ºC-normalised transmembrane flux (J_{20}), 20 ºC-normalised critical flux ($J_{C,20}$), controlled temperature (T), and hydraulic retention time (HRT) in each operating period. J_{20} was studied in MT1 and HRT in the system was controlled with MT2. $J_{C,20}$ determined in MT1 at MLTS of 23 g L^{-1} and SGD_m of 0.23 Nm^3 h^{-1} m^{-2}. N.D.: not determined.

Table 2. Average influent wastewater characteristics.

Table 3. Average sludge characteristics. Nomenclature: **SRB**: sulphate reducing bacteria; **MA**: methanogenic archaea; **SMP**: soluble microbial products; **EPS**: extracellular polymeric substances; **C**: carbohydrates; and **P**: proteins.

Figure 1. Flow diagram of the demonstration plant. Nomenclature: **RF**: rotofilter; **ET**: equalization tank; **AnR**: anaerobic reactor; **MT**: membrane tanks; **DV**: degasification vessel; **CIP**: clean-in-place; **P**: pump; and **B**: blower.

Figure 2. Evolution of membrane permeability and MLTS during the operating period. Experimental period: **(i)** J_{20} at 13.3 LMH and 33 ºC; **(ii)** J_{20} at 10 LMH and 33 ºC; **(iii)** J_{20} at 12 LMH and 25 ºC; and **(iv)** J_{20} at 13.3 LMH and 20 ºC.

Figure 3. Linear dependence of K_{20} upon MLTS and mathematical equation for three of the four experimental series: J_{20} at 13.3 LMH and 33 ºC; J_{20} at 10 LMH and 33 ºC; and J_{20} at 13.3 LMH and 20ºC.

Figure 4. Distribution of mean particle size during the experimental period: **(i)** J_{20} at 13.3 LMH and 33 ºC; **(ii)** J_{20} at 10 LMH and 33 ºC; **(iii)** J_{20} at 12 LMH and 25 ºC; and **(iv)** J_{20} at 13.3 LMH and 20 ºC.

Figure 5. Microscopic observation of mixed liquor at **(a)** mesophilic and **(b)** psychrophilic conditions **(**bar = 100µm).

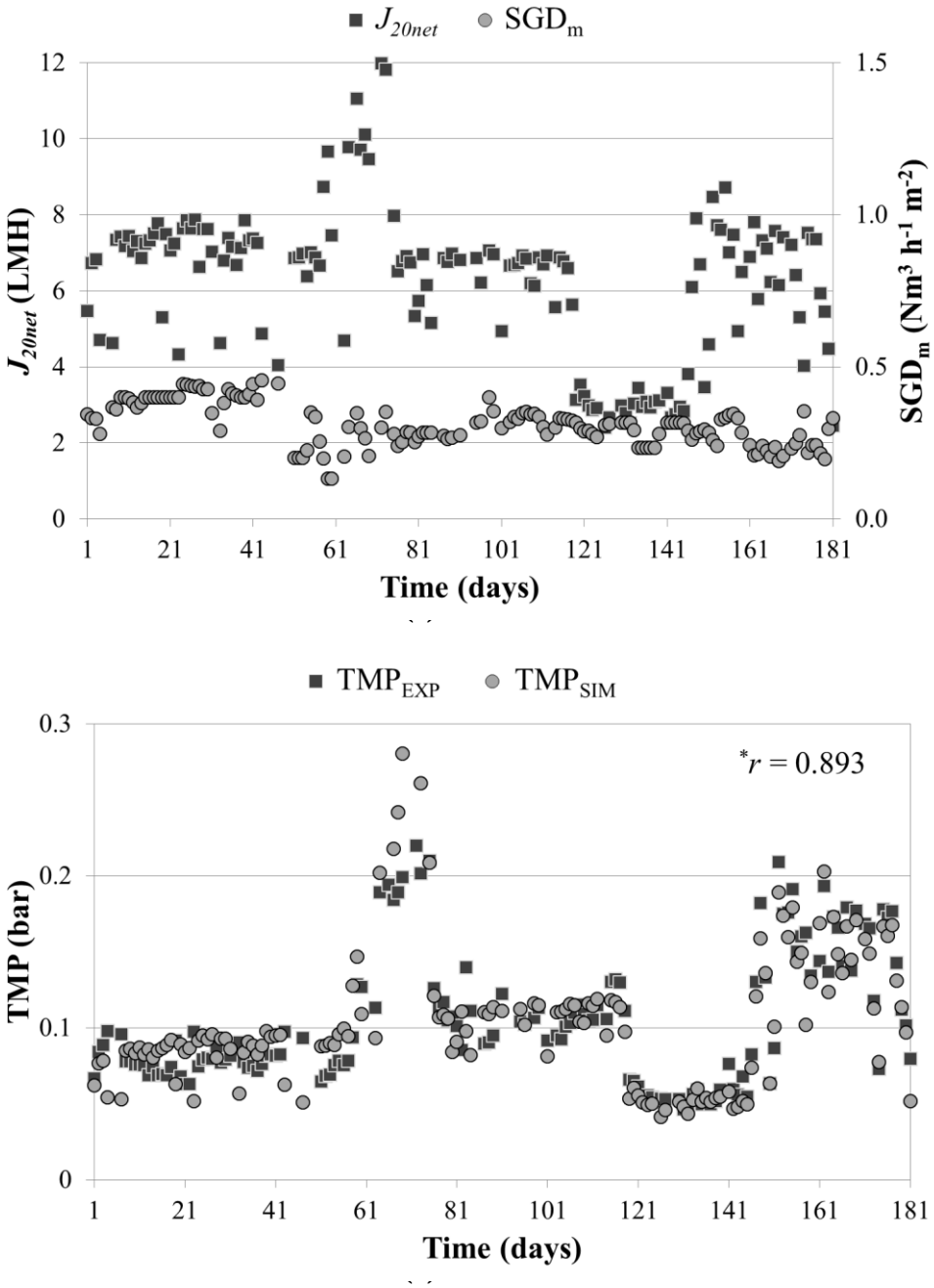

Figure 1. Long-term model validation using heavily-fouled membranes. Daily average values of: **(a)** J_{20} and SGD_m; and **(b)** TMP_{EXP} and TMP_{SIM}. * *r represents the Pearson Product-Moment correlation coefficient between* TMP_{EXP} *and* TMP_{SIM}.

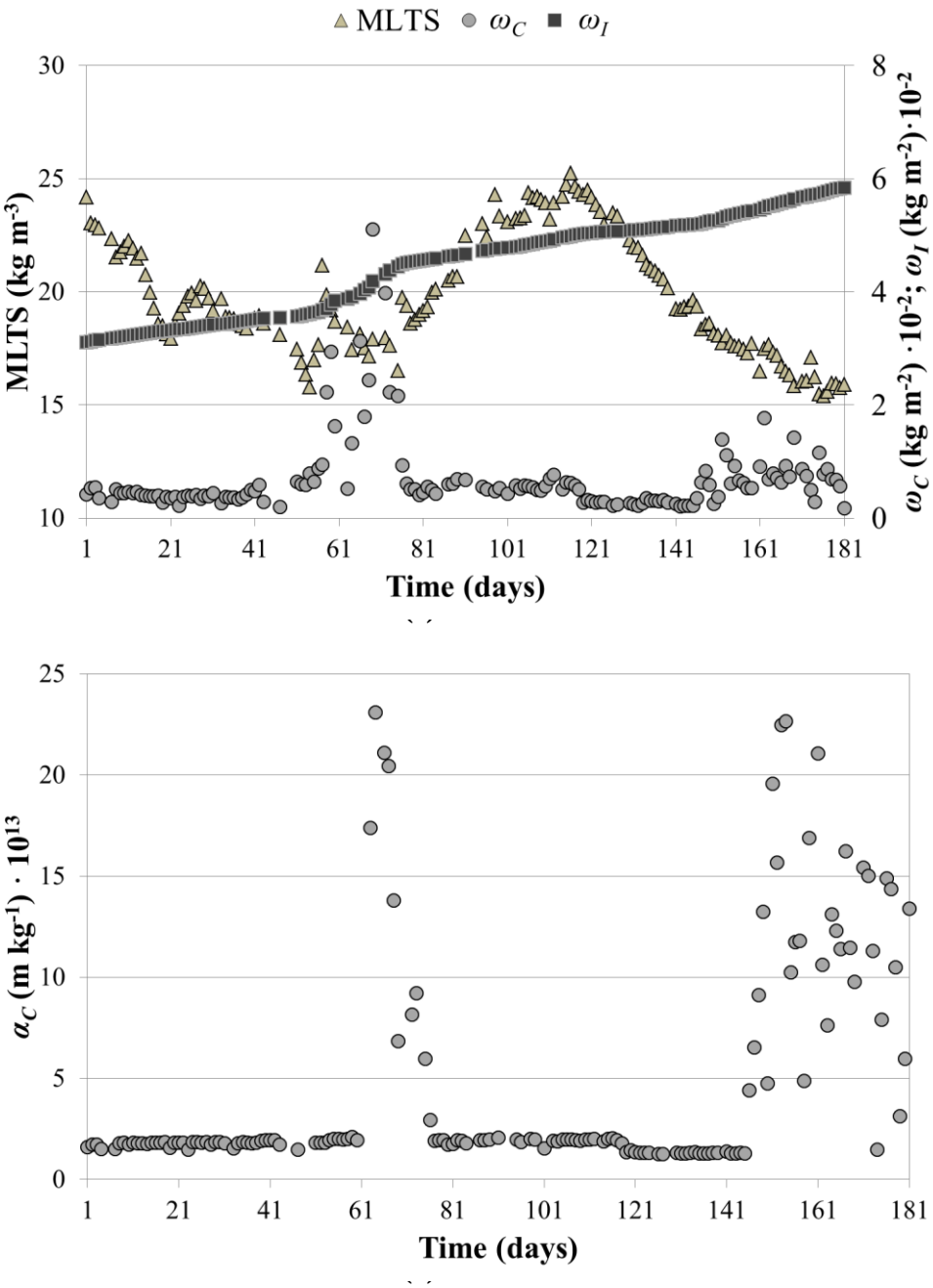

Figure 2. Long-term model validation using heavily-fouled membranes. Daily average values of: **(a)** MLTS, ω_C and ω_I; and **(b)** α_C.

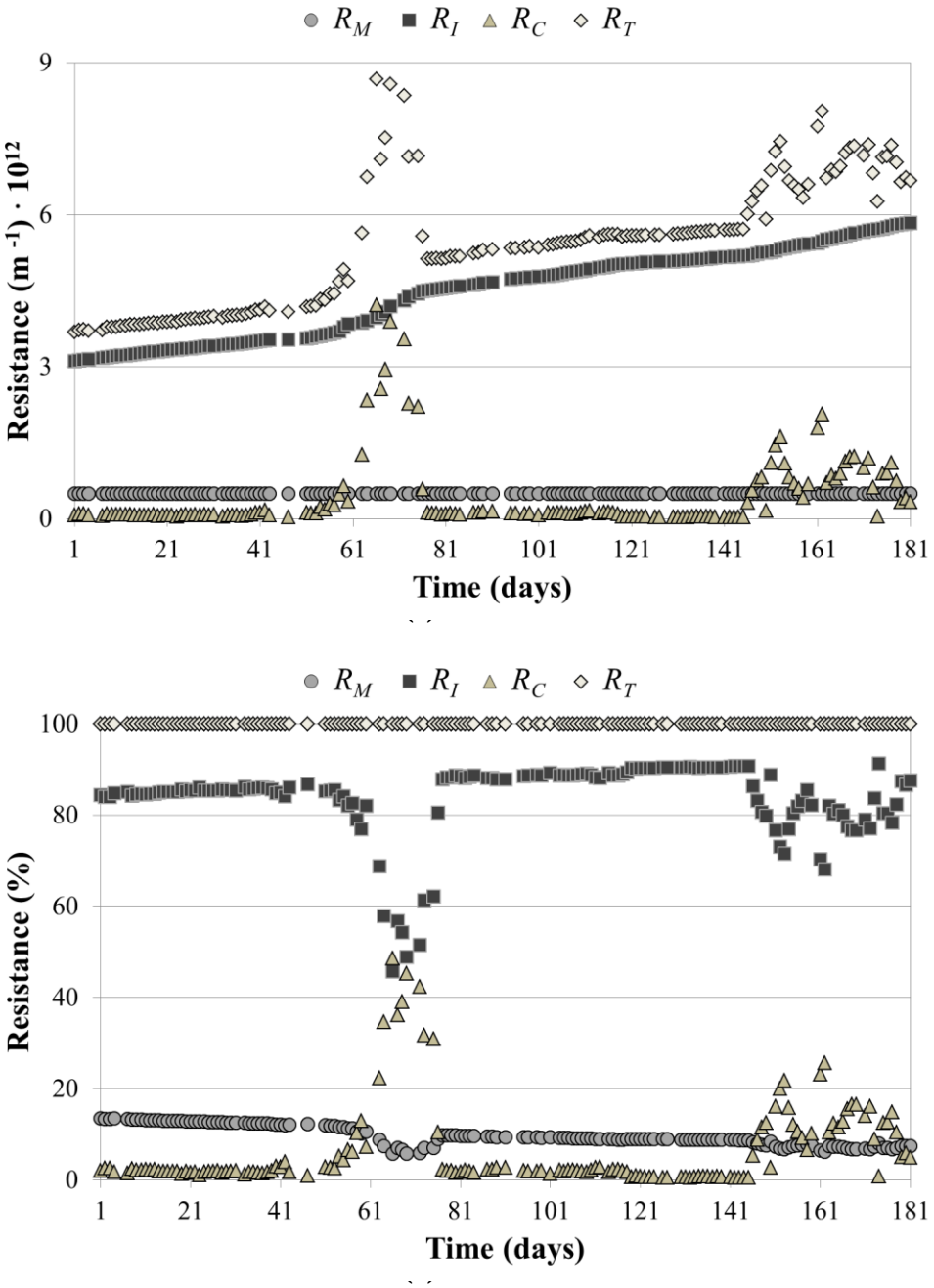

671

672

673

674

675 **Figure 3.** Long-term model validation using heavily-fouled membranes. Daily average values of R_M, R_I,

676 R_C and R_T in: **(a)** absolute terms (m^{-1}); and **(b)** weighted average distribution (%).

677

678

679

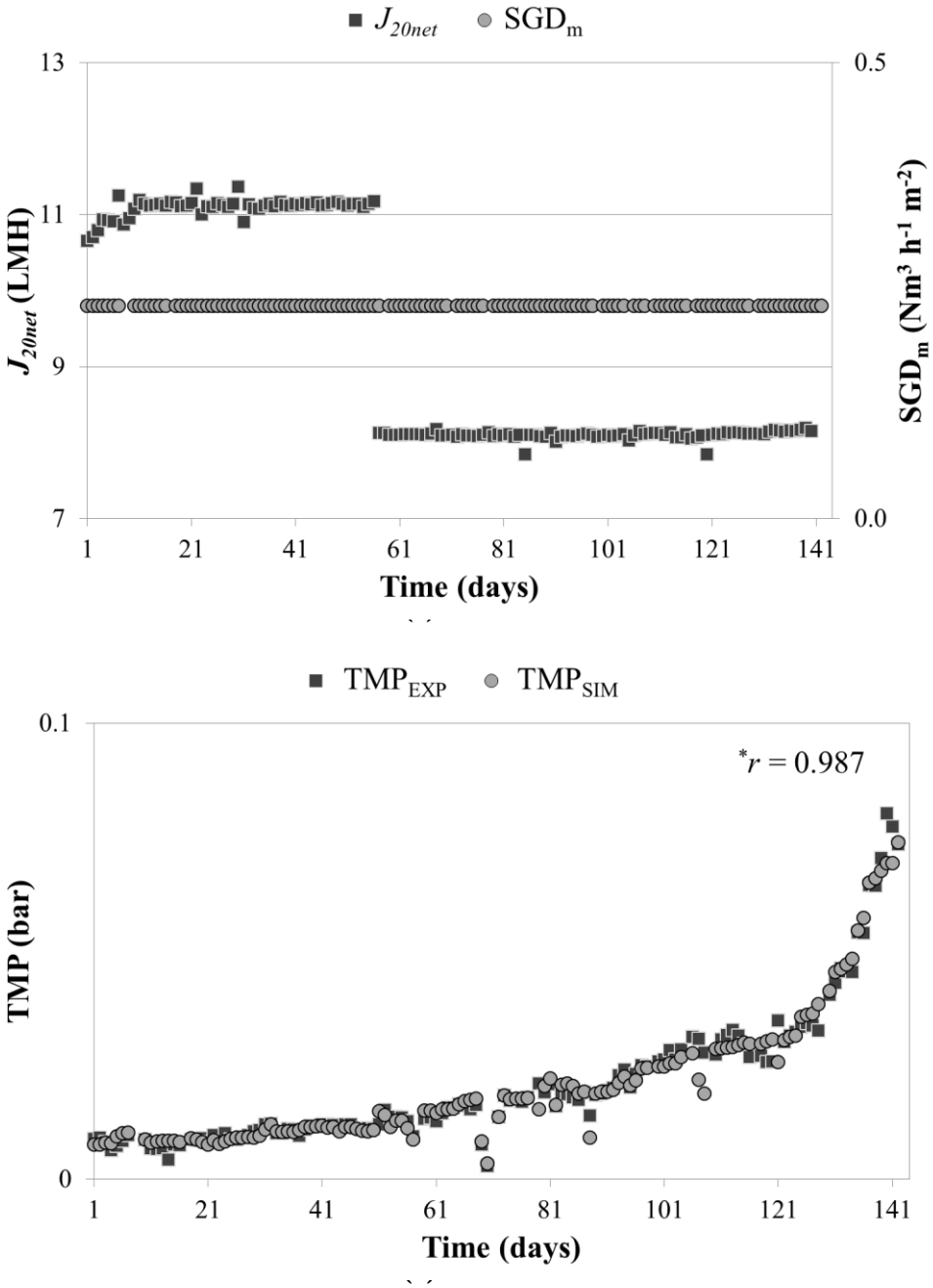

Figure 4. Long-term model validation using lightly-fouled membranes. Daily average values of: **(a)** J_{20} and SGD_m; and **(b)** TMP_{EXP} and TMP_{SIM}. $^*r$ *represents the Pearson Product-Moment correlation coefficient between* TMP_{EXP} *and* TMP_{SIM}.

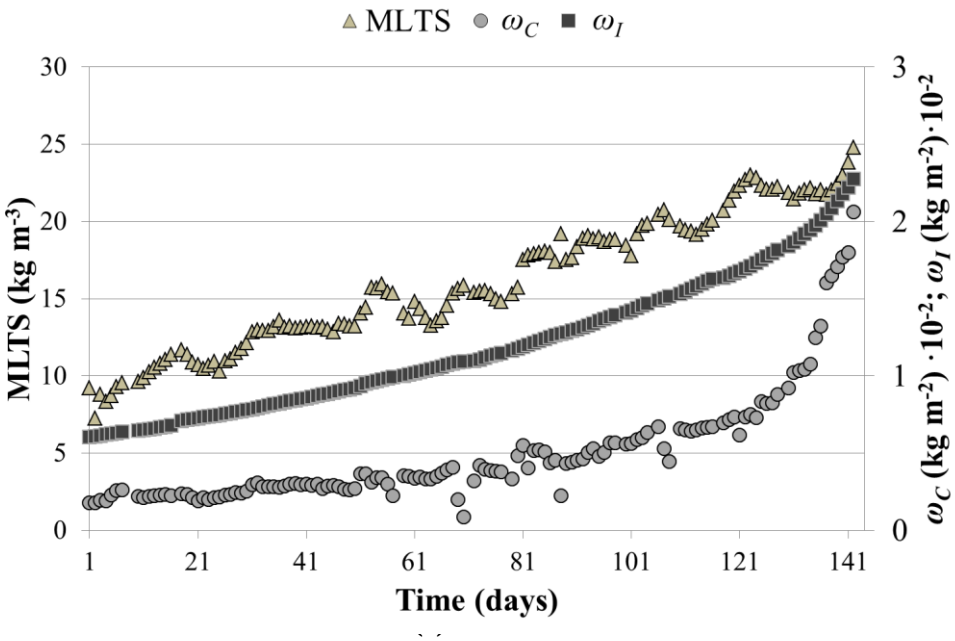

691

692

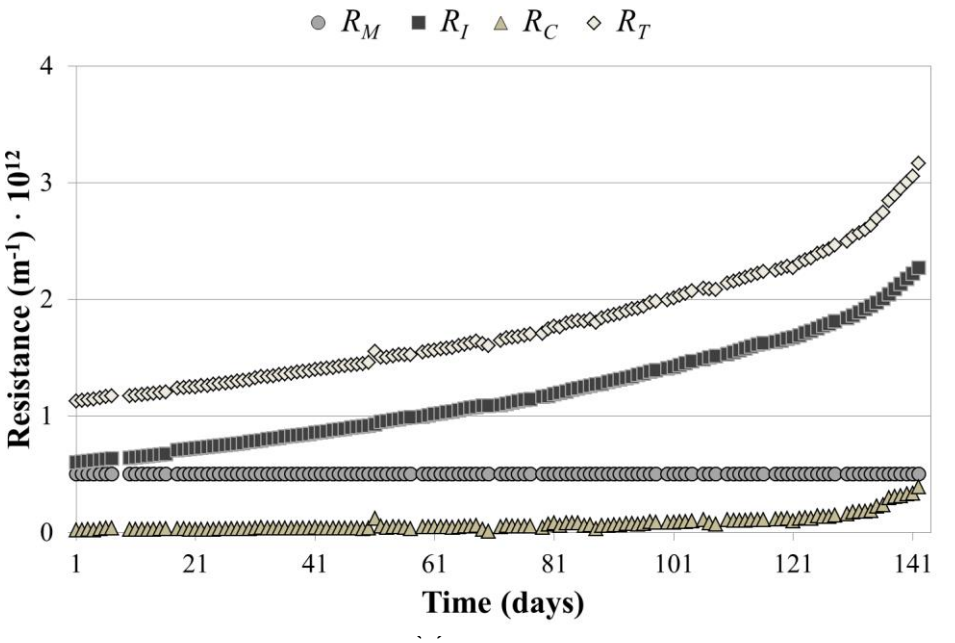

693

694

695 **Figure 5.** Long-term model validation using lightly-fouled membranes. Daily average values of: **(a)**

696 MLTS, ω_C and ω_I; and **(b)** R_M, R_I, R_C and R_T.

697

698

699

700

701

702

703

Table 1. Average values for the 20 ºC-normalised transmembrane flux (J_{20}), 20 ºC-normalised critical flux ($J_{C,20}$), controlled temperature (T), and hydraulic retention time (HRT) in each operating period. J_{20} was studied in MT1 and HRT in the system was controlled with MT2. $J_{C,20}$ determined in MT1 at MLTS of 23 g L^{-1} and SGD_m of 0.23 Nm^3 h^{-1} m^{-2}. N.D.: not determined.

Variable	**Period i** (days 1 to 58)	**Period ii** (days 59 to 170)	**Period iii** (days 171 to 206)	**Period iv** (days 207 to 310)
J_{20} in MT1 (LMH)	13.3	10	12	13.3
$J_{C,20}$ in MT1 (LMH)	N.D.	14	13.5	14
Controlled T (ºC)	33	33	25	20
HRT (h)	16.5	5.5, 9.5, 12	5.5	24.5

728 **Table 2.** Average influent wastewater characteristics.

Parameter	Unit	Mean ± SD
TSS	mgTSS L^{-1}	242 ± 189
VSS	mgVSS L^{-1}	199 ± 148
Total COD	mgCOD L^{-1}	459 ± 263
Soluble COD	mgCOD L^{-1}	81 ± 23
VFA	mgCOD L^{-1}	7 ± 6
SO_4-S	mgS L^{-1}	107 ± 28
NH_4-N	mgN L^{-1}	28.6 ± 9.0
PO_4-P	mgP L^{-1}	3.1 ± 1.3
Alk	mg$CaCO_3$ L^{-1}	309.7 ± 44.8

729
730
731
732
733
734
735
736
737
738
739
740
741
742
743
744
745
746
747
748
749
750
751

752 **Table 3.** Average sludge characteristics. Nomenclature: **SRB**: sulphate reducing bacteria; **MA**:
753 methanogenic archaea; **SMP**: soluble microbial products; **EPS**: extracellular polymeric substances; **C**:
754 carbohydrates; and **P**: proteins.

Parameter	**Unit**	**Mean ± SD**	
		Mesophilic (33 ºC)	**Psychrophilic (20 ºC)**
SRB	%	6 ± 2	3 ± 1
MA	%	4 ± 2	2 ± 1
SRB + MA	%	10 ± 4	5 ± 2
Specific SMP_C	mg g^{-1}MLVS	5 ± 1	2 ± 1
Specific SMP_P	mg g^{-1}MLVS	82 ± 3	14 ± 5
SMP-P/C ratio	mgSMP_P mg$^{-1}SMP_C$	16.4	7.0
$eEPS_C$	mg g^{-1}MLVS	34 ± 4	24 ± 6
$eEPS_P$	mg g^{-1}MLVS	121 ± 9	74 ± 13
eEPS-P/C ratio	mgEPS_P mg$^{-1}EPS_C$	16.4	7.0

755
756
757
758
759
760
761
762